JACS
JOURNAL OF THE AMERICAN CHEMICAL SOCIETY

ARTICLE

pubs.acs.org/JACS

Modeling the Chemical Step Utilized by Human Alkyladenine DNA Glycosylase: A Concerted Mechanism Aids in Selectively Excising Damaged Purines

Lesley R. Rutledge and Stacey D. Wetmore*

Department of Chemistry and Biochemistry, University of Lethbridge, Alberta T1K 3M4, Canada

Supporting Information

ABSTRACT: Human alkyladenine DNA glycosylase (AAG) initiates the repair of a wide variety of (neutral or cationic) alkylated and deaminated purines by flipping damaged nucleotides out of the DNA helix and catalyzing the hydrolytic *N*-glycosidic bond cleavage. Unfortunately, the limited number of studies on the catalytic pathway has left many unanswered questions about the hydrolysis mechanism. Therefore, detailed ONIOM(M06-2X/6-31G(d):AMBER) reaction potential energy surface scans are used to gain the first atomistic perspective of the repair pathway used by AAG. The lowest barrier for neutral 1,N^6-ethenoadenine (εA) and cationic N^3-methyladenine (3MeA) excision corresponds to a concerted (A_ND_N) mechanism, where our calculated $\Delta G^{\ddagger}$ = 87.3 kJ mol^{-1} for εA cleavage is consistent with recent kinetic data. The use of a concerted mechanism supports previous speculations that AAG uses a nonspecific strategy to excise both neutral (εA) and cationic (3MeA) lesions. We find that AAG uses nonspecific active site DNA−protein $\pi-\pi$ interactions to catalyze the removal of inherently more difficult to excise neutral lesions, and strongly bind to cationic lesions, which comes at the expense of raising the excision barrier for cationic substrates. Although proton transfer from the recently proposed general acid (protein-bound water) to neutral substrates does not occur, hydrogen-bond donation lowers the catalytic barrier, which clarifies the role of a general acid in the excision of neutral lesions. Finally, our work shows that the natural base adenine (A) is further inserted into the AAG active site than the damaged substrates, which results in the loss of a hydrogen bond with Y127 and misaligns the general base (E125) and water nucleophile to lead to poor nucleophile activation. Therefore, our work proposes how AAG discriminates against the natural purines in the chemical step and may also explain why some damaged pyrimidines are bound but are not excised by this enzyme.

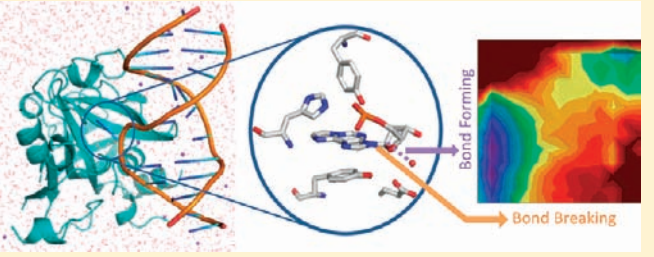

INTRODUCTION

The DNA nucleobases contain an abundant number of nucleophilic sites and are therefore susceptible to reactions with extracellularly and endogenously produced electrophiles.[1−3] This yields a vast array of DNA alkylation lesions, which compromise the well-being of the cell in a variety of ways depending on the type of alkylation damage formed. For example, exposing adenine (A, Figure 1) to methylating agents (such as methylmethanesulfonate (MMS)) or intracellular *S*-adenosylmethionine (SAM) can result in cationic N^3-methyladenine (3MeA, Figure 1).[1−3] While 3MeA is not particularly mutagenic,[3] it is estimated to be produced 600 times per cell per day[4] and is cytotoxic because the methyl group blocks DNA polymerases and stops replication.[2,5] Alternatively, more complex alkylation reactions between the nucleobases and reactive aldehydes generated by industrial agents[1,6] or lipid peroxidation products[7−10] can lead to etheno lesions, such as the adenine analogue 1,N^6-ethenoadenine (εA, Figure 1). This mutagenic lesion has been reported to be present at increased levels in tissues undergoing chronic inflammation[11] and is commonly accepted to increase the risk of colon cancer and liver cancer in Crohn's and Wilson's disease patients, respectively.[12,13]

3MeA and εA are generally repaired through the base excision repair (BER) pathway.[1−3,14−17] A lesion-specific DNA glycosylase initiates this repair process by scanning the DNA strand for damage sites, flipping the nucleotide into the active site, and cleaving the *N*-glycosidic bond that connects the damaged base to the deoxyribose sugar moiety.[18−21] The resulting apurinic/apyrimidinic (AP) site requires subsequent enzymes (such as AP endonuclease, 5′-deoxyribosephosphate lyase, DNA polymerase, and DNA ligase) to fully complete the repair pathway. To date, there is only one DNA glycosylase that has been identified to remove 3MeA and εA lesions in humans, alkyladenine DNA glycosylase (AAG).[3,14−16,22] In fact, AAG is the only human glycosylase known to recognize a wide variety of (neutral and cationic) alkylated and deaminated purines including N^7-methylguanine (7MeG), 1,N^2-ethenoguanine (εG), 1,N^6-ethanoadenine (EA), and hypoxanthine (Hx).[23−30] The enzymatic recognition and removal of diverse lesions is expected to require a nonspecific catalytic mechanism, which comes at the expense of

Received: July 31, 2011
Published: August 30, 2011

dx.doi.org/10.1021/ja207181c | *J. Am. Chem. Soc.* 2011, 133, 16258–16269

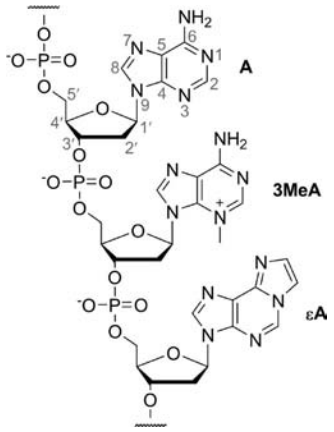

Figure 1. Structure of an oligonucleotide containing adenine (A) and the corresponding DNA alkylation lesions N^3-methyladenine (3MeA) and 1,N^6-ethenoadenine (εA). Atomic numbering of the purine base and sugar moiety is provided in gray.

catalytic power.[26] However, AAG must also have a means to differentiate and exclude the natural nucleobases.[26]

Crystal structures of AAG bound to DNA have revealed vital clues about how this enzyme recognizes and removes damaged lesions.[31−33] X-ray structures of an N-terminally truncated, yet catalytically active, construction of AAG (Δ79AAG) have been bound to a pyrrolidine abasic nucleotide (transition state mimic),[31,32] εA-containing DNA (with E125Q−AAG and a wild-type AAG structure that interestingly left the glycosidic bond intact),[32] and 3, N^4-ethenocytosine (εC)-containing DNA (inhibitor).[33] When AAG binds to εA or εC,[32,33] nonspecific DNA−protein $\pi-\pi$ interactions occur in stacked (Y127) and T-shaped (Y159 and H136) orientations (Figure 2a). As a result, our group has examined the $\pi-\pi$ and $\pi^+-\pi$ interactions between the amino acids with conjugated π-rings and the natural or select damaged nucleobases.[34−37] Our high-level quantum mechanical approach has provided vital information about the preferred structures and stabilization energies of these interactions, as well as how the binding strengths change with respect to several geometric variables. In addition to these $\pi-\pi$ DNA−protein contacts, crystal structures reveal interactions between the backbone N−H of H136 and the N6 site of εA (Figure 2a), as well as the R-group of N169 and C2 of εA,[32] which could yield unfavorable steric contacts with the N6 amino group of adenine (A) and the N2 amino group of guanine (G), respectively. Additional discrimination against the natural purines is provided at the nucleotide-flipping step because stable Watson−Crick pairs are less readily exposed to the active site.[26,38−40] However, it is still not understood how any of the above DNA−protein contacts contribute to the excision of neutral and cationic lesions.

Very little is known about the chemical glycosidic-bond cleavage step catalyzed by AAG, where most of our present knowledge has been revealed from crystal structures of Δ79AAG. A water molecule in the active site is ideally positioned to act as the nucleophile to attack C1′ of the sugar[31−33] (3.502 Å away from C1′ in the wild-type structure bound to εA-containing DNA, Figure 2a).[32] The proximity and orientation of this water relative to the side chain of E125 led to proposals that AAG uses a general base in the catalytic mechanism to activate this water for nucleophilic attack.[31] Indeed, mutational studies that substituted E125 with alanine or glutamine eliminated detectable glycosylase activity, and therefore led to the crystal structure of E125Q−AAG

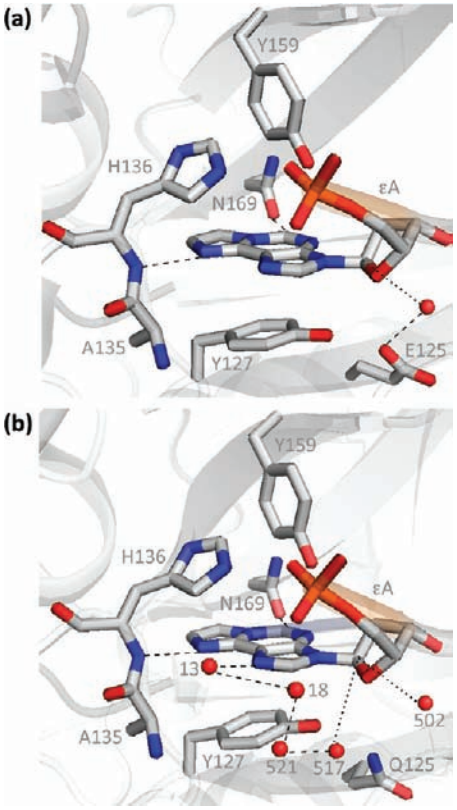

Figure 2. Crystal structure of (a) wild-type Δ79AAG bound to εA-containing DNA (PDB entry 1F4R) and (b) E125Q−Δ79AAG bound to εA-containing DNA (PDB entry 1EWN).[32] Protein-bound water molecules are indicated by red spheres and are labeled according to the crystal structure.

bound to a (glycosidic bond intact) εA-containing DNA (Figure 2b).[32] Additionally, pH−rate profiles clarified that AAG requires a general base for glycosidic-bond cleavage of both neutral (εA, Hx) and cationic (7MeG) substrates,[41] which is also a common feature of most monofunctional glycosylases.[18,19]

O'Brien and Ellenberger found that the pH−rate profiles of the neutral substrates (εA and Hx) are different from the cationic bases (7MeG), suggesting that the neutral lesions require the action of both a general base and a general acid, which protonates the nucleobase.[41] To pinpoint the site of protonation, the activity of AAG toward Hx was compared to that of 7-deaza-Hx, which lacks the N7 group.[41] No glycosylase activity was observed toward 7-deaza-Hx, strongly implying that N7 is directly involved in catalysis of neutral purine lesions.[41] In addition, these authors attempted to identify the general acid by mutating the protein side chains in the vicinity of the bound nucleotide in the εA-containing crystal structure.[41] Unfortunately, the general acid was not identified,[41] and it has yet to be definitively identified.

The above perplexing result led O'Brien and Ellenberger to propose that multiple pathways for protonation of the nucleobase, or perhaps large structural rearrangements from the observed crystal structure, are required to obtain an active complex.[41] Computational work investigating the binding of AAG to εA and EA,[42] or A and Hx,[43] as well as a very recent crystal structure of Δ79AAG bound to εC-containing DNA,[33] observed only minor adjustments in the active site amino acid orientations, and no new candidates for the general acid were identified. However, as

was recently discussed by Samson and co-workers,[33] the crystal structure of E125Q−AAG bound to εA-containing DNA identifies a water molecule in contact with N7 of εA (O_{Wat13}−N7 distance of 2.792 Å, Figure 2b),[32] raising the possibility that a protein-bound water is responsible for protonation. In fact, closer examination of the E125Q−AAG structure bound to εA-containing DNA also reveals a chain of protein-bound water molecules connecting the proposed general acid located near N7 of εA (Wat13) to Wat517, which is 3.479 Å from C1′ of the sugar moiety (Figure 2b), and raises the potential for a water-mediated glycosidic-bond cleavage mechanism. Upon overlaying the εA-[32] and εC-containing[33] crystal structures, the location of Wat13 with respect to the εC inhibitor led Samson and co-workers to propose that the failure of AAG to cleave εC, as well as other pyrimidines, could be due to the inability of AAG to activate the leaving group by protonation.[33] Despite these proposals, computational and mass spectrometry studies by Lee and co-workers spark interesting questions about the commonly accepted general acid mechanism for excision of neutral lesions.[44,45] Specifically, comparisons of the (N7) proton affinities and (N9) acidities of the Hx[44] and εA[45] substrates to the natural purines A and G reveal that protonation by a general acid is not necessary for cleavage. In fact, these data suggest that AAG would have a more discriminatory chemical step in the absence of a general acid mechanism.

To date, no study has united all of the computational and experimental results presented above to fully describe the mechanism-of-action of AAG. With this goal in mind, the present work uses ONIOM(QM:MM) calculations to examine the chemical step utilized by AAG to cleave the glycosidic bond in εA, 3MeA, and A nucleotides. Potential energy surfaces (PES) are generated to consider the complete reaction paths and determine whether the reaction is stepwise or concerted for different (neutral or cationic) lesions. The substrate choices allow us to assess the dependence of the chemical step on the charge of the substrate and, perhaps more importantly, whether the glycosidic-bond cleavage mechanism provides an extra step for AAG to discriminate against the natural purines. Furthermore, our methodology will elucidate the role of a general acid in the excision of neutral lesions by considering crystal structure orientations of protein-bound water molecules near N7 of the purines, as well as different water nucleophiles, which takes into account possible water chain proton transfer reactions. For comparisons with experiment, as well as to help clarify the role of the amino acids with conjugated π-rings (H136, Y127, Y159), mutational analysis is used to determine how active site residues affect the activation energy of the hydrolysis reaction for both neutral and cationic substrates. Through this work, we propose a chemical mechanism for AAG that is consistent with all previous experimental and computational results, provides insights into the role played by various amino acids in the cleavage step for neutral and cationic substrates, and suggests how AAG discriminates against the natural purines at this late stage in the mechanism-of-action.

COMPUTATIONAL METHODS

Initial Model Generation. The X-ray structure of the E125Q AAG/εA−DNA complex (1EWN PDB entry[32]) was used as the starting point for this study. The R-group of amino acid residues that were not resolved in the crystal structure (H82, E131, T199, V208, K210, Q238, E240, and E269) was first added with the Leap program.[46,47] Hydrogen atoms were then added to the DNA−protein system, which was neutralized with sodium ions and fully solvated with 8650 water molecules in a TIP3P water box to yield a 8 Å water buffer around the system and a total box size of 69 Å × 69 Å × 71 Å. The εA substrate present in this crystal structure was assigned AMBER[48] atom types and GAFF[49] parameters using ANTECHAMBER[50] (shown in Figure SI-1 and Table SI-1 in the Supporting Information). The original charges for εA were obtained using the RESP (restrained electrostatic potential)[51,52] program, which fits the partial atomic charges to the ESP grid generated in a (gas-phase) HF/6-31G(d) calculation on the (M06-2X/6-31G(d) hydrogen-atom optimized) crystal structure orientation of the nucleotide. All other residues were initially assigned AMBER charges.[48]

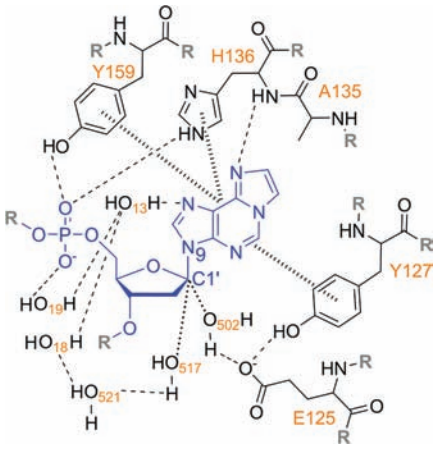

Figure 3. Schematic representation of the QM region used in ONIOM (M06-2X/6-31G(d):AMBER) calculations for the εA substrate (blue). Link atoms (represented by hydrogen atoms in M06-2X/6-31G(d) calculations) are indicated by R (in bold).

In the present work, a two-layer (mechanical embedding) ONIOM (our own *N*-layer integrated molecular orbital molecular mechanics) method[53−55] in Gaussian 09[56] was used for all QM/MM calculations, which has recently become an important technique for computational studies of enzymatic catalysis (see, for example, refs 57−71). Active site residues (εA7 nucleotide substrate, Q125, Y127, A135, H136, Y159, Wat13, Wat18, Wat19, Wat502, Wat517, Wat521) were included in the QM region (78 heavy atoms) and were described with M06-2X/6-31G(d) (Figure 3). Previous work from our group compared the performance of 12 density functional theory (DFT) methods with double-ζ basis sets to 129 gold-standard (CCSD(T)/CBS) DNA−protein stacked and T-shaped interaction energies and determined that M06-2X provides an overall excellent description of both types of π−π interactions.[72] Additionally, M06-2X was originally developed to provide an excellent performance for main-group thermochemistry and kinetic applications.[73] The rest of the system was described with molecular mechanics (MM) using the parm96 parameters of the AMBER force field.[48]

The (solvated) system was initially optimized with MM in two stages; first, all noncrystallographic atoms were relaxed, and then the MM region was relaxed with the QM region fixed. Afterward, the entire QM region was relaxed to a fixed MM region within the ONIOM methodology. To reduce the computational cost for the remaining ONIOM calculations, the noncrystallographic water and counterions were removed at this stage, and residues more than 15 Å from the glycosidic bond were held fixed in this geometry. The relaxed system was mutated to generate the active form of AAG (E125 replaced Q125, where the AMBER charges for E were used[48]) and then optimized using the ONIOM scheme outlined above. The εA nucleobase in this reactant was subsequently mutated to be adenine (A) or N^3-methyladenine (3MeA) (RESP charges for the new nucleotides were obtained through HF/6-31G(d)

calculations on the (M06-2X/6-31G(d)) hydrogen-atom optimized nucleotides, where 3MeA atom types and parameters are reported in Figure SI-1 and Table SI-1), and the new enzyme−substrate complexes were optimized within the ONIOM scheme.

Finally, to obtain the fully relaxed reactants, the partial charges of the QM region were converged with the procedure developed by Schlegel and co-workers.[61,74] Specifically, after the initial ONIOM optimization, an improved set of (gas-phase HF/6-31G(d)) RESP charges was calculated for the entire (hydrogen-atom capped) QM region using the newly optimized structure, and an additional ONIOM optimization was performed. This procedure was repeated until convergence was achieved, which required that both the difference between the total ONIOM energies from the two last rounds of optimization calculations as well as the difference between the total ONIOM energies in the first and last optimization steps in the final optimization calculation be less than 4 kJ mol^{-1}. While this typically required 6−10 rounds of optimization, in a few cases where both convergence criteria could not be achieved after more trials, one criterion was required to be less than 2 kJ mol^{-1}. Convergence in this manner ensures that the QM charges are conserved along the entire reaction path.[61,74]

Reaction Potential Energy Surface Generation. Reaction potential energy surfaces (PES) were obtained by constraining the glycosidic (C1′−N9) and nucleophilic (C1′−O_{wat}) distances in the above reactants, where both Wat502 and Wat517 were considered as the nucleophile for all three substrates (Figure 3). All points on each PES were obtained by constraining the two grid coordinates and minimizing the energy with respect to the remaining parameters. For each point, the geometry was optimized with the quadratically coupled QM/MM optimizer as implemented in Gaussian 09.[56] Once a converged structure was obtained for a given point on the PES, new RESP charges for the optimized QM region were calculated (as outlined by Schlegel and co-workers[61,74]) and used in an ONIOM single-point calculation to obtain the final reported energy. Additionally, the charges and coordinates from this single-point calculation were altered to create the starting guess for the optimization of the next point on the PES, where only one reaction coordinate was changed at a time in 0.200 Å increments. This process was repeated until all stationary points on the preferred reaction surfaces were identified.

Further Refinement of Stationary Points. The geometries of all stationary points identified from the preferred reaction surfaces were further refined in two manners. First, to obtain the constrained stationary points, the C1′−N9 and C1′−O_{wat} distances were kept fixed, while the RESP charges of the QM region were fully converged as described above for the reactant structures. Second, to obtain the relaxed stationary points, the charges for the QM region were fully converged while releasing the C1′−N9 and C1′−O_{wat} distance constraints. All stationary points (constrained and relaxed) were confirmed to be minima and transition states through frequency calculations, where the one imaginary frequency found for each transition state was visually inspected to verify that it corresponds to the proper reaction coordinate. To obtain the Gibbs free energy, the corresponding (unscaled) thermal correction obtained from the frequency was added to the ONIOM energy of the complex, which uses standard statistical mechanics expressions for an ideal gas in the canonical ensemble.

Point Mutations. Mutations of Y127, H136, and Y159 (specifically, Y127A, H136A, and Y159A) were performed to determine the role of the active site amino acid residues in the cleavage of the glycosidic bond of εA and 3MeA. Additionally, Y127W and Y159W mutations were considered for the εA substrate to allow for comparison to experimentally measured[40,41] changes in the wild-type barrier height. To ensure that our stationary points did not collapse upon optimization, only constrained wild-type stationary points (C1′−N9 and C1′−O_{wat502} distances held fixed) were considered.[75] Mutations of wild-type residues to alanine were generated by replacing Cγ with a hydrogen atom and removing any additional atoms of the original R-group, while mutations to tryptophan were generated by positioning the new R-group to best resemble the orientation recently proposed by O'Brien and co-workers.[40] The coordinates of only the new residue were first optimized, and then the QM region was allowed to relax while keeping the entire MM region fixed. The charges of the QM region were then fully converged to allow comparison to the (wild-type) constrained stationary points, and frequency calculations were completed to confirm the nature of stationary points and obtain Gibbs free energy corrections. We note that our choice in mutational structures allows us to determine the (local) energetic effects of the mutation on the barrier rather than the (global) structural and energetic effects considered in experimental mutational studies. Because of the lack of structural information available for these mutations, we feel that this comparison is arguably the best approach to isolate the contribution of each residue to the barrier corresponding to the wild-type mechanism.

RESULTS

Through careful consideration of the crystal structure of E125Q−AAG bound to εA-containing DNA (PDB entry 1EWN[32]), reaction coordinates corresponding to the glycosidic-bond cleavage (C1′−N9) and the nucleophilic water addition (C1′−O_{wat}) were chosen to construct a series of reaction PES. Specifically, for each substrate considered (εA, 3MeA, A), two water molecules (Wat502 and Wat517) were investigated as the nucleophile in the reaction because both waters are in close proximity to C1′. In particular, Wat502 is closer to E125 (general base), while Wat517 is connected to neutral substrates through a water chain to Wat13 (Figure 2b). For both nucleophile choices, Wat13 is able to protonate the neutral substrates, even though leaving-group activation is not explicitly forced through our choice of reaction coordinates. Details of the ONIOM(QM:MM) PES and refined stationary points will be presented for each substrate individually, and subsequently point mutation results for both neutral and cationic substrates will be discussed.

1,N^6-Ethenoadenine (εA) Substrate. The PES for excision of the εA substrate using Wat502 or Wat517 as the nucleophile is shown in Figure 4a (relative energies in Table SI-2) and b (relative energies in Table SI-3), respectively. In both plots, the bottom left region contains the reactant (R), which has a glycosidic-bond distance of 1.500 Å, and C1′−O_{wat} nucleophile distance of 3.200 or 3.000 Å for the Wat502 or Wat517 nucleophile, respectively. When Wat502 acts as the nucleophile, a concerted transition state (TS) occurs at a C1′−N9 distance of 2.300 Å and C1′−O_{wat502} distance of 2.200 Å, while a dissociative TS is found for Wat517 (located at a C1′−N9 distance of 3.300 Å and C1′−O_{wat517} distance of 3.000 Å). The concerted transition state on the Wat502 surface is much lower in energy (by 38%) than the dissociative TS found for Wat517, implying that Wat502 is a more likely nucleophile for the glycosidic-bond cleavage mechanism. Therefore, completion of the entire PES for the reaction involving Wat517 was deemed unnecessary, and this potential nucleophile was not further considered. For the Wat502 nucleophile, the endothermic product (P) is located at a C1′−N9 distance of 3.500 Å and C1′−O_{wat502} distance of 1.400 Å. Gibbs free energy calculations were also completed for all points on the Wat502 surface (Figure SI-2), which revealed that the location of stationary points and general surface contours are not affected. Therefore, the Gibbs free energy surface was only considered for the εA substrate.

To ensure QM charges are conserved along the entire reaction path, the RESP charges for the stationary points identified on the

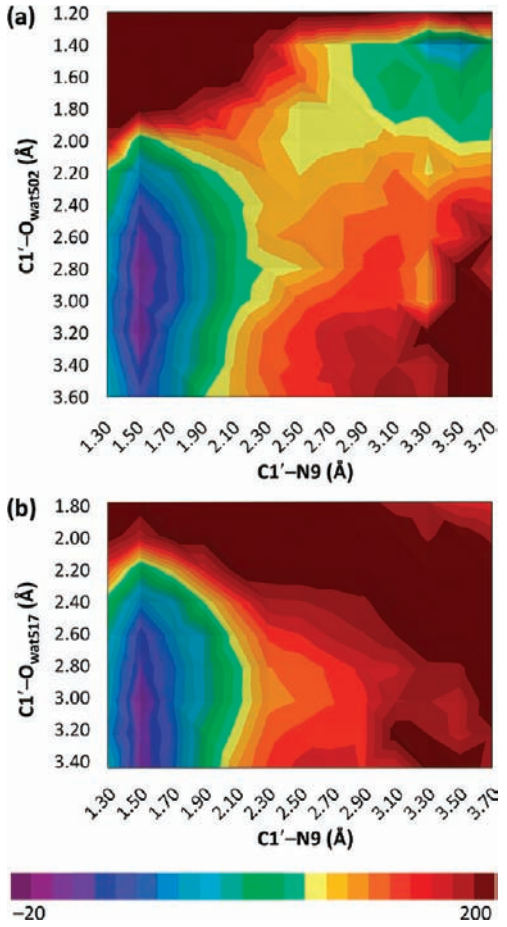

Figure 4. Reaction surfaces for the glycosidic-bond (C1′−N9) cleavage in the εA nucleotide by AAG using (a) Wat502 or (b) Wat517 as the nucleophile. The ONIOM(M06-2X/6-31G(d):AMBER) energies (ΔE, kJ mol^{-1}) are reported relative to the respective reactant, where each color band reflects a 10 kJ mol^{-1} energy contour.

Wat502 PES were fully converged while maintaining fixed reaction coordinates (constrained (Table 1 and Figure SI-3)) or relaxing these reaction coordinates (relaxed (Table 1 and Figure 5)). The geometry of the relaxed reactant is very similar to the constrained reaction coordinate distances, with the exception that the water nucleophile (Wat502) moves further from C1′ (3.356 Å) to be more consistent with the crystal structure distance (3.613 Å).[32] The flipped-out nucleotide adopts the C3′-*exo* sugar puckering observed in the crystal structure, which is maintained throughout the reaction. The nucleobase−protein $\pi-\pi$ interactions slightly change from the original crystal structure orientation, but are consistent across all (constrained and relaxed) stationary points. Specifically, Y127 and H136 are more tightly bound in our relaxed reactant than the crystal structure[32] (by 0.335 and 0.399 Å, respectively) and are more planar with respect to the nucleobase (12.1° and 40.3° become 4.1° and 7.7°, respectively).[76] It is expected that this difference is at least in part due to the M06-2X functional slightly overbinding $\pi-\pi$ interactions;[77] however, deviations could also arise because comparisons are being made to a crystal structure, which represents an average geometry. By considering the TS complexes, the reaction barrier decreases by 5.2 kJ mol^{-1} when the distance constraints are removed, due to a slight increase in the glycosidic-bond distance (0.110 Å) and a small decrease in the nucleophile distance (0.087 Å). Nevertheless, the relaxed TS is consistent with a concerted mechanism as determined from the original PES. The endothermic product binds more tightly to the sugar moiety when the reaction coordinates are relaxed (by 0.619 Å), leading to a decrease in the reaction energy by 19.4 kJ mol^{-1}.

Table 1. Relative Energies (ΔE) and Gibbs Free Energies (ΔG) for the Concerted Mechanism Used by AAG To Excise the εA and 3MeA Substrates[a]

	εA				3MeA			
	constrained[b]		relaxed[c]		constrained[b]		relaxed[c]	
	ΔE	ΔG	ΔE	ΔG	ΔE	ΔG	ΔE	ΔG
TS	101.3	88.9	96.1	87.3	75.0	62.1	70.6	57.9
P	58.4	75.4	39.0	43.5	−98.0	−26.2	−19.1	−21.9

[a] ONIOM(M06-2X/6-31G(d):AMBER) energies are reported in kJ mol^{-1} and are relative to the corresponding reactant. [b] The C1′−N9 and C1′−O$_{wat502}$ distances were held fixed, but the RESP charges for the QM region were fully converged. See the Computational Methods. [c] No distance constraints were enforced, and the RESP charges for the QM region were fully converged. See the Computational Methods.

The geometric changes as the reaction progresses can be observed in Figure 6. Proceeding from the ONIOM(M06-2X/6-31G(d):AMBER) relaxed R to TS, the εA base tilts away from the sugar in a relatively unchanged active site (Figure 6a) to maintain a similar water chain around the nucleotide (Figure 6b). Interestingly, the angles between the molecular planes of the nucleobase and active site amino acid rings (Y127, H136, and Y159) increase as a result of the more tilted nucleobase in the TS geometry (Figures 5 and 6c). The hydrogen-bonding distance between Wat13 and the N7 site of εA decreases from the R to the TS by 0.143 Å, but proton transfer does not occur at any stage of the reaction. Transfer of the nucleophilic water (Wat502) proton to the general base (E125) does not happen until after the transition state. Following proton transfer from the nucleophile, the hydrogen-bond stabilization originally provided to E125 by Y127 is replaced by Wat517 (Figure 5), which results in a tightly bound water chain in the product (Figure 6b). Interestingly, this water chain orientation is optimally positioned to regenerate the active form of this enzyme.

***N*^{3}-Methyladenine (3MeA) Substrate.** When 3MeA is placed in the active site of AAG and Wat517 is considered as a nucleophile, the resulting PES is too high in energy to be viable, and a much more realistic PES is determined when C1′−O$_{wat502}$ is one of the reaction coordinates (Figure 7a and Table SI-4). The corresponding reactant is located at a C1′−N9 distance of 1.500 Å and a C1′−O$_{wat502}$ distance of 3.200 Å. The lowest energy transition state corresponds to a concerted pathway (C1′−N9 = 2.300 Å and C1′−O$_{wat502}$ = 2.600 Å), where a (15.5 kJ mol^{-1}) slightly higher in energy, more dissociative TS occurs at C1′−N9 = 2.700 Å and C1′−O$_{wat502}$ = 3.000 Å. The overall reaction is exothermic with the product located at a C1′−N9 distance of 3.300 Å and C1′−O$_{wat502}$ distance of 1.400 Å.

Similarly to εA, the stationary points identified from the 3MeA excision PES were refined by converging the charges of the QM region while constraining the two reaction coordinates (constrained (Table 1 and Figure SI-4)) or relaxing the two constraints (relaxed (Table 1 and Figure 8)). The structures of these stationary points are in good agreement, where the (concerted) reaction barrier decreases by only 4.4 kJ mol^{-1} when the stationary points are fully

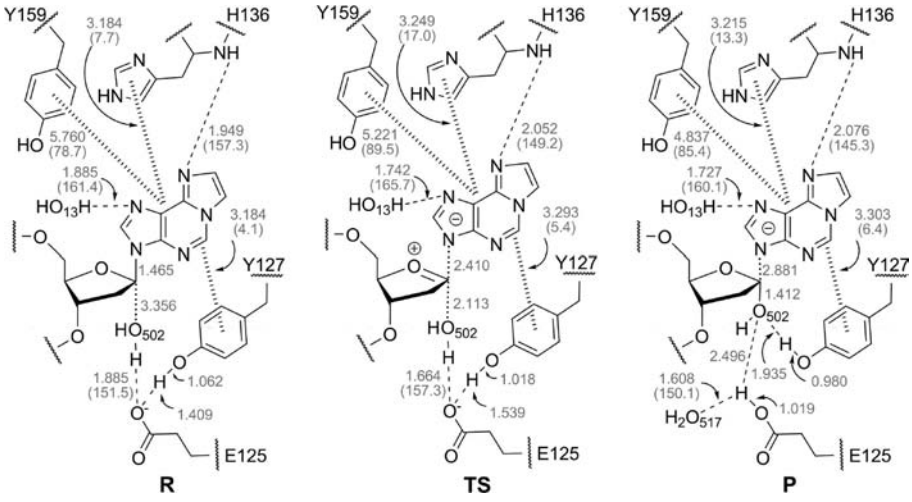

Figure 5. Important ONIOM(M06-2X/6-31G(d):AMBER) structural information (hydrogen-bond distances in Å (angles in degrees and in parentheses)) for the fully relaxed stationary points for the excision of εA by AAG.[76]

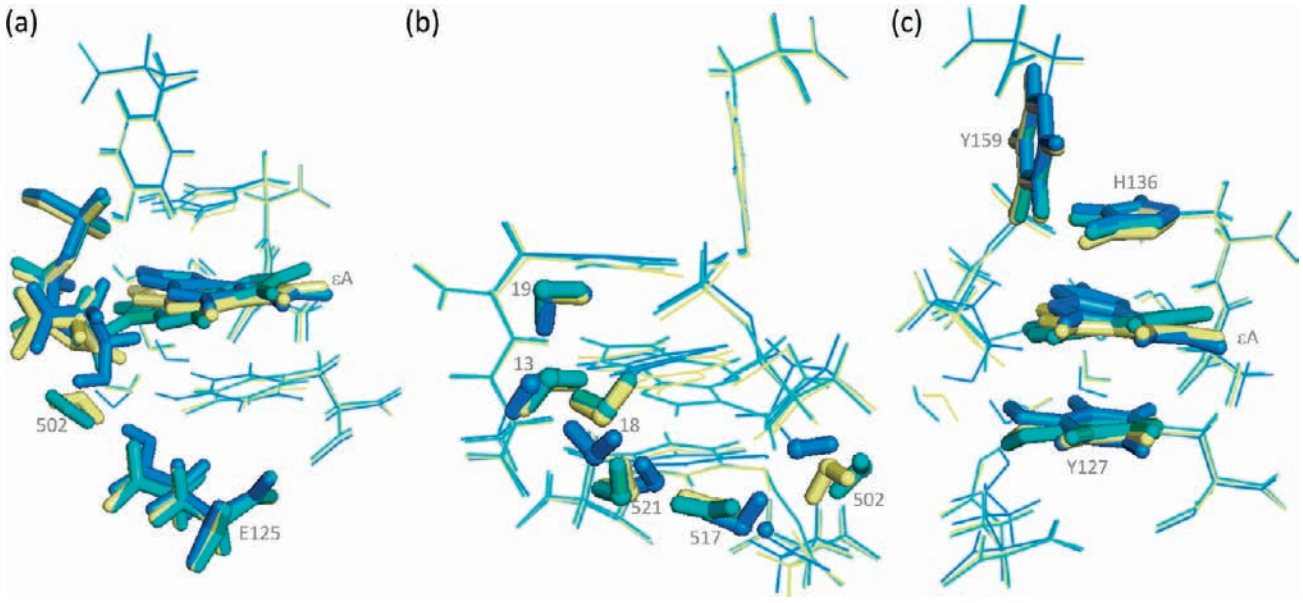

Figure 6. Overlay of the QM regions from relaxed ONIOM(M06-2X/6-31G(d):AMBER) calculations for excision of εA by AAG, where the structure shown in green corresponds to the reactant, yellow to the transition state, and blue to the product. Tube representations highlight the (a) εA substrate, nucleophilic water molecule (Wat502), and the general base (E125), (b) active site water molecules, and (c) $\pi-\pi$ interactions between the εA nucleobase and Y127, H136, and Y159.

relaxed (glycosidic-bond distance increases by 0.254 Å and nucleophile distance decreases by 0.248 Å). The barrier height for the excision of 3MeA is 25.5 kJ mol^{-1} (ΔG is 29.4 kJ mol^{-1}) lower in energy than that for the εA reaction, which results from the inherently destabilized glycosidic bond in the cationic lesion.[78,79] The relaxed product binds more tightly to the sugar moiety, but is less exothermic than the corresponding constrained stationary point.

Large structural changes occur in the active site of AAG upon binding of a cationic alkylation lesion. For example, Wat13 reorients and interacts with the backbone nitrogen of A135 instead of the N7 site of neutral εA (Figure 9). Additionally, the backbone N−H of H136 that is directed toward the N6 site of εA rearranges to form a hydrogen bond between the N6 amino group of 3MeA and the carbonyl oxygen in the backbone of A135 (Figure 9). Indeed, the 3MeA reactant is more tilted in the active site relative to the DNA backbone (the χ ($\angle$(O4′−C1′−N9−C4)) dihedral angle is 173.1° as compared to 180.5° for εA) to maximize the interactions between the A135 backbone and the hydroxyl group of Y159 ($O_{Y159}-H_{3MeA}$ distance with a N^3-methyl group hydrogen atom of 3MeA is 2.270 Å). Furthermore, the DNA−protein $\pi-\pi$ interactions between 3MeA and Y127 or H136 are less planar and more spatially separated than observed for εA, while the opposite is true for Y159 (Figure 5 and Figure 8). Despite these ONIOM(QM:MM) structural differences, the PES for both the εA and the 3MeA substrates contains a hydrogen bond between the general base (E125) and Y127 before nucleophile (Wat502) proton transfer occurs, which is after the TS in both reactions.

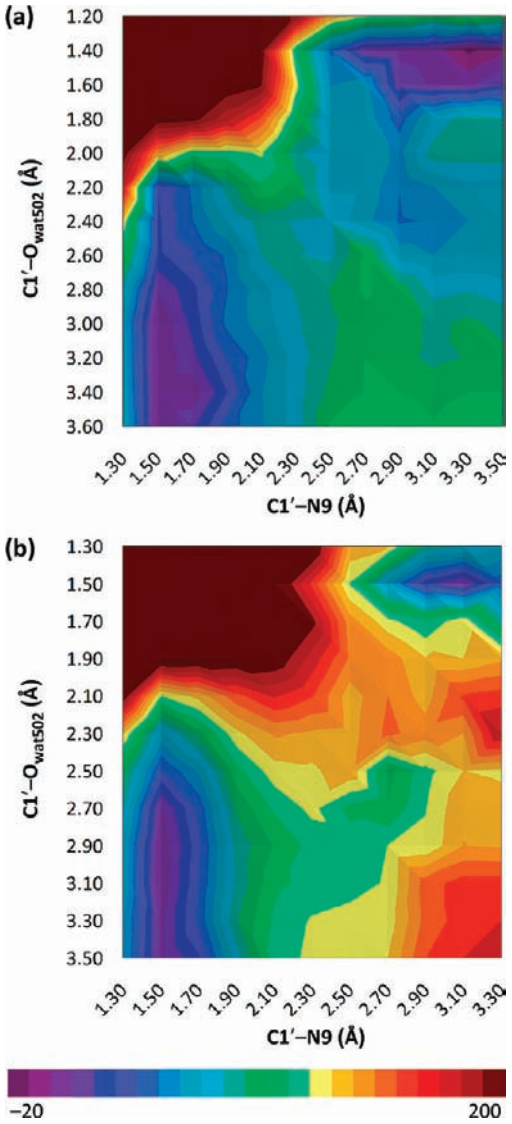

Figure 7. Reaction surfaces for the glycosidic-bond (C1′−N9) cleavage mechanism in the (a) 3MeA and (b) A nucleotides by AAG using Wat502 as the nucleophile. The ONIOM(M06-2X/6-31G(d):AMBER) energies (ΔE, kJ mol^{-1}) are reported relative to the respective reactant, where each color band reflects a 10 kJ mol^{-1} energy contour.

Adenine (A) Substrate. The only energetically feasible adenine excision pathway occurs when Wat502 is the nucleophile (Figure 7b and Table SI-5). Therefore, as is true for all of the substrates examined in this study, a protein-bound water chain that connects C1′ to the Wat13 molecule located near N7 of neutral substrates is not used to cleave the glycosidic bond. The adenine reactant occurs at a glycosidic-bond distance of 1.500 Å and nucleophile distance of 3.100 Å. However, unlike the surfaces calculated with εA and 3MeA, the lowest energy TS is dissociative and occurs at C1′−N9 = 2.500 Å and C1′−O$_{wat502}$ = 2.900 Å. This leads to an intermediate at glycosidic and nucleophilic distances of 2.700 and 2.500 Å, respectively. As the nucleophilic water molecule associates toward C1′, another transition state (glycosidic distance of 2.900 and nucleophilic distance of 2.300 Å) occurs before the slightly endothermic product is formed (C1′−N9 = 3.100 Å and C1′−O$_{wat502}$ = 1.500 Å). The PES also reveals a higher-energy (22.9 kJ mol^{-1}) concerted TS at glycosidic and nucleophilic distances of 2.300 and 2.300 Å, respectively.

When the charges for the QM region are fully converged for the constrained stationary points (Table 2 and Figure SI-5), a stepwise (D_N*A_N) mechanism is confirmed because the concerted barrier is 23.5 kJ mol^{-1} (ΔG of 20.6 kJ mol^{-1}) higher in energy than the dissociative barrier. However, this preferred mechanism for A bond cleavage is still 17.4 kJ mol^{-1} (ΔG of 18.6 kJ mol^{-1}) higher in energy than the (concerted) barrier height for εA. Full relaxation of the A stationary points was unsuccessful due to large fluctuations in the water chain within the active site. However, the constrained stationary points reveal that the N6 amino group of adenine puckers away from the backbone N−H of H136 throughout the reaction (C5−C6−N6−H6 dihedral angle ranges from 41.6° (dissociative TS) to 66.6° (R)) to reduce steric clashes. As the nucleobase dissociates from the sugar, the N7 site maximizes a hydrogen bond with Wat13 and the backbone N−H bond of H136 (Figure SI-5). The π-containing active site amino acids bind closer to A as compared to εA, where slightly tilted interactions with Y127 and H136 in the reactant become much more planar as the reaction proceeds (Figure SI-5). Even more intriguing is the disappearance of the stabilizing hydrogen bond between Y127 and the general base (E125) in the A reactant (Figures 10 and SI-5). Instead, Wat517 simultaneously donates a hydrogen bond to E125 and accepts a hydrogen bond from Y127 in the stationary points prior to nucleophilic proton transfer (Figures 10 and SI-5).

Point Mutations. Using constrained stationary points, a mutational analysis was conducted to better understand the involvement of various amino acids in the excision of neutral and cationic alkylation lesions (εA and 3MeA, Table 3). Specifically, Y127A, H136A, and Y159A mutations were examined to provide insights into the energetic effects of removing active site π-systems on the bond cleavage barrier for neutral and cationic lesion excision. These point mutations increase the wild-type εA barrier height by 11.7 (H136A), 15.9 (Y159A), or 27.5 kJ mol^{-1} (Y127A). Contrary to the εA results, these mutations for the 3MeA substrate result in a very small effect (0.7 kJ mol^{-1} increase in barrier for Y159A) or a significant decrease in the reaction barrier (by up to 38.1 kJ mol^{-1}). In addition, Y127W and Y159W were examined with εA to allow for comparison of our calculated (energetic) mutational results (Table 3) to recently reported (chemical step) reaction barriers.[40] The Y127W mutation was found to have a larger effect on the wild-type barrier height (30.9 kJ mol^{-1}) than the Y159W mutation (27.2 kJ mol^{-1}).

DISCUSSION

Excision of εA by Wild-Type, Y127W, and Y159W AAG Agrees with Experiment. This Article presents the first atomic level description of the chemical step used by AAG. Our detailed ONIOM(QM:MM) calculations reveal that a concerted mechanism is used to excise εA with a 96.1 kJ mol^{-1} reaction barrier ($\Delta G^{\ddagger}$ = 87.3 kJ mol^{-1}). A very recent study measured single turnover rate constants and is the only work, to the best of our knowledge, that reports a barrier corresponding to the glycosidic-bond cleavage step of εA excision.[40] Excellent agreement between experimental (90.7 kJ mol^{-1})[40] and computational barriers provides strong support for our computational approach. Indeed, this comparison suggests that our calculations can contribute detailed chemical insights into other aspects of the chemical mechanism of AAG with confidence.

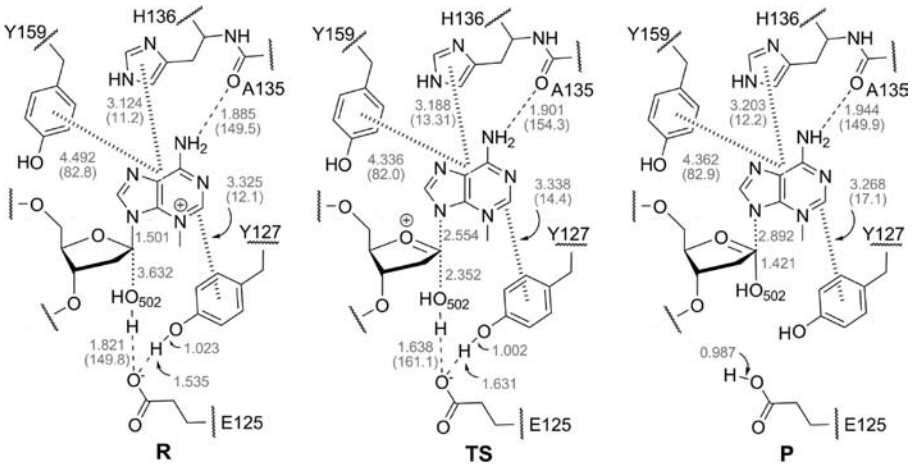

Figure 8. Important ONIOM(M06-2X/6-31G(d):AMBER) structural information (hydrogen-bond distances in Å (angles in degrees and in parentheses)) for the fully relaxed stationary points for the excision of 3MeA by AAG.[76]

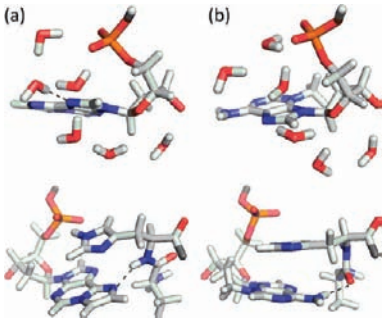

Figure 9. Relaxed ONIOM(M06-2X/6-31G(d):AMBER) reactants for the (a) εA and (b) 3MeA substrates, highlighting the interactions between the substrate and active site water molecules (top), and the substrate, A135 and H136 (bottom).

Table 2. Relative Energies (ΔE) and Gibbs Free Energies (ΔG) for the Excision of A by AAG[a]

	A	
	constrained[b]	
	ΔE	ΔG
TS[c]	137.0	126.5
$TS_{dissociative}$[d]	113.5	105.9
I[d]	110.3	98.5
$TS_{associative}$[d]	126.3	111.9
P	34.9	34.5

[a] ONIOM(M06-2X/6-31G(d):AMBER) energies are reported in kJ mol^{-1} and are relative to the corresponding reactant. [b] The C1′−N9 and C1′−O_{wat502} distances were held fixed, but the RESP charges for the QM region were fully converged. See the Computational Methods. [c] The transition state along a concerted pathway. [d] Corresponds to a stepwise mechanism where the base first dissociates from the sugar ($TS_{dissociative}$) to form an intermediate (I), and then association of the nucleophilic water molecule ($TS_{associative}$) occurs.

The recent kinetic study mentioned above also examined the effects of substituting the two active site tyrosine residues with tryptophan on the nucleotide flipping and base excision steps.[40] It was determined that the Y127W and Y159W mutant proteins have robust excision activity toward εA-containing DNA ($\Delta G^{\ddagger}$ of 94.0 and 92.8 kJ mol^{-1}, respectively).[40] Although our calculated $\Delta G^{\ddagger}$ barriers for these two mutations are indistinguishable, the energetic result of these mutations increases the calculated wild-type $\Delta E^{\ddagger}$ to 132.2 and 128.5 kJ mol^{-1} for Y127W and Y159W, respectively (Table 3). Indeed, our mutational analysis predicts the experimentally observed trend that Y127 plays a more important role in chemical catalysis for εA excision, which will be further discussed below. We acknowledge that the calculated local energetic contribution of these mutations is larger than the global (energetic and structural) contributions observed through experiment. Although better agreement is expected upon full relaxation of our system, this would require full PES scans to identify appropriate stationary points, which were deemed unnecessary because the effects of tyrosine mutations are not the focus of the current study. Nevertheless, our reasonable match further verifies the ability of our approach to properly describe this enzymatic mechanism.

AAG Prefers an S_N2 (A_ND_N) Mechanism for Excision of Both Neutral and Cationic Lesions. Because the catalytic mechanism of AAG is currently unknown, the chemical mechanism must be conjectured by considering the corresponding nonenzymatic depurination reactions[80−91] and other enzymatic hydrolysis reactions.[18,19,84,92,93] Experimental studies of spontaneous depurination[80−83,85,86,88] and the reactions catalyzed by other monofunctional DNA glycosylases (uracil DNA glycosylase (UDG)[92] and MutY DNA glycosylase (MutY)[93]) support a dissociative ($D_N{}^*A_N$) *N*-glycosidic-bond cleavage mechanism, which results in a transition state with a positive charge accumulated on C1′ and O4′ of the sugar moiety and little association of the water nucleophile.[18,19] Further support for a dissociative hydrolysis mechanism is gained from the ability of positively charged abasic DNA analogues (4-azaribose and 1-azaribose), which mimic an oxacarbenium ion-like transition state, to function as tight-binding inhibitors of AAG.[41,94] However, crystal structures indicate that a more associative mechanism (such as a concerted (A_ND_N) mechanism) may be favored by AAG because the nonspecific active site may be unable to stabilize a wide variety of leaving groups, and the nucleophilic water is tightly positioned between the general base and the anomeric carbon.[18] Furthermore, there is no reason to believe that this enzyme would exploit the same mechanism as the corresponding nonenzymatic

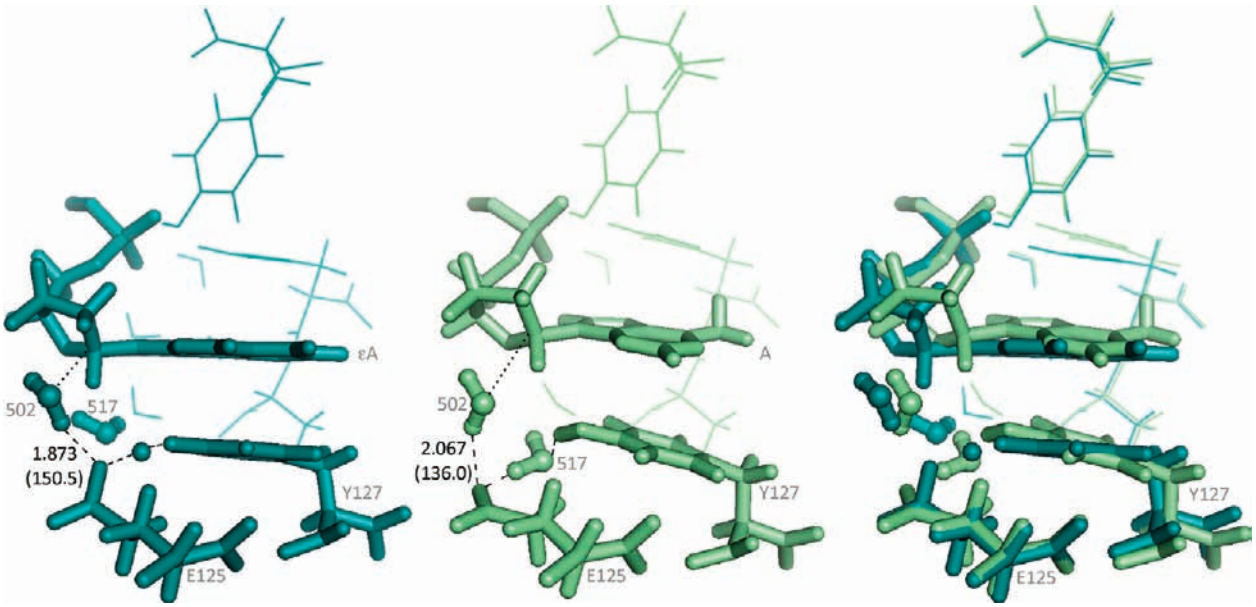

Figure 10. QM regions from constrained ONIOM(M06-2X/6-31G(d):AMBER) reactants for excision of εA (dark green) and A (light green) by AAG. Tube representations highlight the substrate, nucleophilic water molecule (Wat502), the general base (E125), Wat517, and Y127, where the nucleophilic activation hydrogen-bond distances (Å) and angles (degrees, in parentheses) are also reported.

Table 3. Calculated Barrier Heights and Changes in Barrier Heights from Single-Point Mutations of AAG with the εA and 3MeA Substrates[a]

	εA		3MeA	
	ΔE	ΔG	ΔE	ΔG
wild-type	101.3	88.9	75.0	62.1
H136A	113.0 (11.7)	111.4 (22.5)	36.9 (−38.1)	28.2 (−33.9)
Y127A	128.8 (27.5)	118.5 (29.6)	53.9 (−21.1)	45.1 (−17.0)
Y159A	117.2 (15.9)	107.6 (18.7)	75.7 (0.7)	61.9 (−0.2)
Y127W	132.2 (30.9)	124.5 (35.6)		
Y159W	128.5 (27.2)	124.6 (35.7)		

[a] ONIOM(M06-2X/6-31G(d):AMBER) barrier heights are reported relative to the reactant (in kJ mol^{-1}). Changes in the barrier heights (in parentheses) are reported relative to the wild-type barrier, where a positive value represents an increase in barrier height upon mutation.

reaction.[93] Indeed, many enzymes, such as thymidine phosphorylase[95] and some *O*-glycosidases,[96] stabilize transition states that are drastically different from the uncatalyzed (*N*- or *O*-glycosidic-bond cleavage) reactions.

Examination of the complete reaction surfaces for the εA and 3MeA substrates suggests that AAG prefers to excise both (neutral and cationic) lesions through a concerted (A_ND_N) mechanism. In fact, one benefit of performing detailed reaction PES scans is that a concerted mechanism is revealed to be preferred over the dissociative ($D_N{}^*A_N$) mechanism by over 20 or 15 kJ mol^{-1} for the εA and 3MeA substrates, respectively. Therefore, our results elucidate that AAG uses a concerted (A_ND_N) chemical step as a nonspecific strategy to excise both neutral (εA) and cationic (3MeA) lesions. Indeed, a mechanistic strategy that is not specific to the chemical composition or charge of the lesion excised may be vital in the mechanism-of-action of this promiscuous DNA glycosylase.

$\pi-\pi$ Interactions Contribute Differently to the Excision of Neutral and Cationic Lesions. To better understand the role of the individual DNA−protein $\pi-\pi$ interactions found in the active site of AAG, the catalytic contribution of each amino acid π-system to the excision of neutral (εA) and cationic (3MeA) lesions was investigated. Specifically, Y127A, H136A, and Y159A mutations were considered as discussed in the Computational Methods. Despite previous proposals that $\pi-\pi$ interactions could be anticatalytic for neutral base excision,[18] our calculations indicate that the π-systems of Y127, H136, and Y159 favorably contribute to catalysis by lowering $\Delta G^{\ddagger}$ by 29.6, 22.5, and 18.7 kJ mol^{-1}, respectively (Table 3). We note that the calculated contribution of these amino acid π-systems provides information about how the barrier increases after removing both hydrogen-bonding and $\pi-\pi$ interactions from the active site; however, due to the difficulties associated with separating these contributions, further mutational analysis was not considered.[97] On the contrary, Y127, H136, and Y159 were found to negligibly affect or be anticatalytic toward the excision of 3MeA by increasing the $\Delta G^{\ddagger}$ by 17.0, 33.9, and 0.2 kJ mol^{-1}, respectively. These results are consistent with our previous high-level ab initio findings that the $\pi^+-\pi$ stacking and T-shaped interactions between 3MeA and histidine or tyrosine can be up to 135% more stabilizing than the corresponding $\pi-\pi$ interactions involving A.[35,36] Taken together, this suggests that the anticatalytic contribution of these conjugated π-rings is due to overbinding of the cationic reaction complex.

In addition to clarifying the role of the active site π-containing amino acid residues, which is different for the neutral and cationic substrates, our work reveals for the first time how AAG balances between mechanistic specificity and catalytic power.[26] Specifically, it appears that AAG has evolved to take advantage of the amino acid π-systems to nonspecifically position a wide variety of alkylation damage products in the active site, while at the same time maximizing catalytic power toward (neutral) lesions that are inherently more difficult to excise. Although the ability to also

remove neutral DNA damage comes at the expense of the excision rate for the repair of cationic lesions, stronger attraction and binding of cationic lesions is achieved through enhanced $\pi-\pi$ contacts[35,36] as AAG processively searches the DNA strand for damage.[98,99]

A General Acid Contributes to Neutral Base Excision through Hydrogen-Bond Donation. To investigate the recently proposed possibility that a protein-bound water molecule is responsible for protonation of neutral substrates,[33] our QM/MM model unbiasedly incorporated Wat13 such that hydrogen bonding to, or protonation of, the N7 site of neutral substrates (εA or A) was not explicitly forced. Although Wat13 was found to donate a hydrogen bond to N7 of εA throughout the excision reaction (Figure 5), no proton transfer to N7 occurs. Interestingly, deletion of Wat13 from the εA mechanism results in an increase in $\Delta G^{\ddagger}$ of 28.9 kJ mol^{-1},[100] which suggests hydrogen-bond donation or only partial protonation is enough to catalyze this reaction. This finding challenges the generally accepted protonation mechanism, which is a common, but not universal, feature of enzymatic purine hydrolysis reactions.[101,102] However, closer examination of the original study that proposed the role of this general acid reveals that hydrogen-bond donation to the neutral base can also explain the observed pH−rate profile.[41] Furthermore, our observation is consistent with the experimental and computational work by Lee and co-workers, who suggested AAG will excise εA and Hx without nucleobase protonation because greater (weaker) N9 acidities (N7 proton affinities) make these lesions easier to excise (harder to protonate) than the natural purines.[44,45] Interestingly, despite the large proton affinity of the N7 site of A,[44,45] only hydrogen-bond stabilization with Wat13 was observed throughout the A excision mechanism (Figure SI-5). Therefore, although we support suggestions that a general acid mechanism is important for the excision of neutral substrates, we propose that hydrogen-bond donation from the general acid provides enough stabilization to lower the excision barrier. This is consistent with mechanistic proposals for UDG, where a neutral histidine residue unambiguously stabilizes the uracil leaving group only through hydrogen-bond donation.[18]

AAG Also Uses the Chemical Step To Discriminate Against the Natural Purines. AAG is just one example of a broadly specific enzyme that employs a weaker catalytic mechanism to process many different lesions, and yet avoids intolerable excision of substrates that are essential to cell function.[26] The nucleotide-flipping step used by AAG provides discrimination against the natural bases because they are less readily exposed to the enzyme active site.[26,38] Crystal structures also reveal that H136 and N169 in the AAG active site provide unfavorable interactions with the exocyclic amino groups of A and G, respectively.[32] However, it is currently unknown whether these interactions are enough to prevent excision of the natural purines. Therefore, it was essential for the current study to also examine the excision of A by this promiscuous enzyme.

Our calculations indicate that excision of A is higher in energy and proceeds in a different manner than the excision of the neutral lesion εA. By comparing the stationary points of the A substrate to those of εA, we can obtain insights into why these energetic and mechanistic differences are observed. Specifically, a stabilizing hydrogen bond between the hydroxyl group of Y127 and the carbonyl of the general base (E125) is present in both the εA and the 3MeA surfaces, but not for A. Instead, Wat517 donates a hydrogen bond to E125 (accepts from Y127) in the stationary points that occur before nucleophilic proton transfer on the A surface (Figure 10). An overlay of the εA and A reactants reveals that A is inserted further into the active site of AAG (Figure 10), which allows the active site water chain to move closer to Y127 and form the new hydrogen bond. As a result of this hydrogen-bond rearrangement, E125 in the A reactant reorients to be further from C1′, which moves the water nucleophile (Wat502) further from the general base, and, perhaps more importantly, Wat502 is poorly aligned for nucleophile activation. Indeed, Wat502 is misaligned throughout the entire reaction mechanism of A (Figure SI-5), which results in a large barrier for water association (Figure 7b). Therefore, this work indicates for the first time that Y127 not only provides stabilization to E125,[32] but also plays a larger role in orienting E125 for effective nucleophile activation. Additionally, one of our most important findings is that AAG can use the chemical step to discriminate against the natural bases by potentially misaligning and poorly activating the nucleophilic water molecule.

Support for our new proposal that E125 plays a key role in aligning the nucleophilic water molecule is gained from the experimentally measured decrease in activity of the E125Q and E125A mutants toward εA.[41] Specifically, this suggests that the catalytic contribution from the general base is larger than expected for chemical activation of a nucleophile participating in a dissociative glycosidic-bond cleavage reaction.[41] Our calculated concerted transition state could explain this larger catalytic contribution of E125 than that expected for a more dissociative mechanism. Additionally, these mutational experiments suggest that E125 may play an important role in positioning the nucleophilic water for attack at the anomeric carbon of the substrate.[41] In fact, our current work shows that the general base (E125) plays a very important role in activating the water nucleophile by orienting the water molecule for the concerted excision mechanism of its preferred substrates and accepting the proton from the water nucleophile in the late stages of this reaction. In addition to this newly identified role for E125, our calculations are consistent with the generally accepted function of this general base to stabilize the cationic charge formed on the sugar moiety in the transition state of most glycosylase excision reactions.[18,19]

Investigations of a recent crystal structure with the εC inhibitor bound to Δ79AAG led to a proposal that εC is not excised by AAG because the leaving group cannot be activated through protonation.[33] However, our results indicate that protonation is not necessary for glycosidic-bond cleavage to occur. Despite the fact that poor nucleophilic water activation was dismissed as the reason for low glycosylase activity toward εC,[33] this crystal structure only provides an atomistic perspective of one point on the potential energy surface. In light of our current results, we believe this structure actually provides further evidence for the proposed importance of nucleophile alignment because, like A, εC is further inserted into the catalytically active binding site of AAG.[33] Therefore, our computational results across the entire reaction surface indicate that AAG uses the chemical step as yet another discriminatory strategy to prevent excision of the natural purines.

Our calculations demonstrate that detailed QM/MM reaction PES scans can provide valuable information about the energy landscape of glycosylase reactions, which can be difficult to explicitly examine through other means. More importantly, this study helps clarify how AAG uses nonspecific $\pi-\pi$ DNA−protein interactions to catalyze the removal of inherently more difficult to excise neutral lesions, and strongly attract and bind the

cationic lesions, which comes at the expense of raising the excision barrier for repair of cationic substrates. In fact, our mechanistic investigation provides insight into how AAG has a large substrate tolerance that is well suited to protecting DNA from alkylation damage while limiting excision of unmodified bases. It is expected that future studies that further describe the complete mechanistic strategy of this enzyme, including substrate binding and nucleotide flipping, will be vital for explaining similar promiscuous enzymes that appear throughout chemical biology.

■ ASSOCIATED CONTENT

Supporting Information. AMBER atom types and GAFF parameters, tables of energies for the PES plots, comparison of ΔE and ΔG surface plots for εA substrate, important structural information for constrained stationary points for all three substrates, optimized QM region coordinates (full QM/MM coordinates available upon request), energies for all stationary points, and complete refs 46, 47, and 56. This material is available free of charge via the Internet at http://pubs.acs.org.

■ AUTHOR INFORMATION

Corresponding Author
stacey.wetmore@uleth.ca

■ ACKNOWLEDGMENT

Computational resources from the Upscale and Robust Abacus for Chemistry in Lethbridge (URACIL) and those provided by Westgrid and Compute/Calcul Canada are greatly appreciated. We thank the Natural Sciences and Engineering Research Council of Canada (NSERC), the Canadian Research Chair Program, and the Canadian Foundation for Innovation (CFI) for financial support. L.R.R. acknowledges NSERC (CGS-D), Alberta Innovates — Technology Futures, the Government of Alberta, and the University of Lethbridge for student scholarships.

■ REFERENCES

(1) Drablos, F.; Feyzi, E.; Aas, P. A.; Vaagbo, C. B.; Kavli, B.; Bratlie, M. S.; Pena-Diaz, J.; Otterlei, M.; Slupphaug, G.; Krokan, H. E. *DNA Repair* **2004**, *3*, 1389–1407.
(2) Sedgwick, B. *Nat. Rev. Mol. Cell Biol.* **2004**, *5*, 148–157.
(3) Shrivastav, N.; Li, D. Y.; Essigmann, J. M. *Carcinogenesis* **2010**, *31*, 59–70.
(4) Rydberg, B.; Lindahl, T. *EMBO J.* **1982**, *1*, 211–216.
(5) Fronza, G.; Gold, B. *J. Cell. Biochem.* **2004**, *91*, 250–257.
(6) Barbin, A. *Mutat. Res., Rev. Mutat. Res.* **2000**, *462*, 55–69.
(7) Elghissassi, F.; Barbin, A.; Nair, J.; Bartsch, H. *Chem. Res. Toxicol.* **1995**, *8*, 278–283.
(8) Chung, F. L.; Chen, H. J. C.; Nath, R. G. *Carcinogenesis* **1996**, *17*, 2105–2111.
(9) Marnett, L. J. *Carcinogenesis* **2000**, *21*, 361–370.
(10) Marnett, L. J. *Toxicology* **2001**, *164*, 18–18.
(11) Bartsch, H.; Nair, J. *Cancer Detect. Prev.* **2002**, *26*, 308–312.
(12) Coussens, L. M.; Werb, Z. *Nature (London, U. K.)* **2002**, *420*, 860–867.
(13) Nair, U.; Bartsch, H.; Nair, J. *Free Radical Biol. Med.* **2007**, *43*, 1109–1120.
(14) Wyatt, M. D.; Allan, J. M.; Lau, A. Y.; Ellenberger, T. E.; Samson, L. D. *BioEssays* **1999**, *21*, 668–676.
(15) Gros, L.; Ishchenko, A. A.; Saparbaev, M. *Mutat. Res.* **2003**, *531*, 219–229.
(16) Sedgwick, B.; Bates, P. A.; Paik, J.; Jacobs, S. C.; Lindahl, T. *DNA Repair* **2007**, *6*, 429–442.
(17) Rubinson, E. H.; Gowda, A. S. P.; Spratt, T. E.; Gold, B.; Eichman, B. F. *Nature (London, U. K.)* **2010**, *468*, 406–U309.
(18) Stivers, J. T.; Jiang, Y. L. *Chem. Rev.* **2003**, *103*, 2729–2759.
(19) Berti, P. J.; McCann, J. A. B. *Chem. Rev.* **2006**, *106*, 506–555.
(20) O'Brien, P. J. *Chem. Rev.* **2006**, *106*, 720–752.
(21) Friedman, J. I.; Stivers, J. T. *Biochemistry* **2010**, *49*, 4957–4967.
(22) Plosky, B.; Samson, L.; Engelward, B. P.; Gold, B.; Schlaen, B.; Millas, T.; Magnotti, M.; Schor, J.; Scicchitano, D. A. *DNA Repair* **2002**, *1*, 683–696.
(23) Engelward, B. P.; Weeda, G.; Wyatt, M. D.; Broekhof, J. L. M.; deWit, J.; Donker, I.; Allan, J. M.; Gold, B.; Hoeijmakers, J. H. J.; Samson, L. D. *Proc. Natl. Acad. Sci. U.S.A.* **1997**, *94*, 13087–13092.
(24) Hang, B.; Singer, B.; Margison, G. P.; Elder, R. H. *Proc. Natl. Acad. Sci. U.S.A.* **1997**, *94*, 12869–12874.
(25) Abner, C. W.; Lau, A. Y.; Ellenberger, T.; Bloom, L. B. *J. Biol. Chem.* **2001**, *276*, 13379–13387.
(26) O'Brien, P. J.; Ellenberger, T. *J. Biol. Chem.* **2004**, *279*, 9750–9757.
(27) Vallur, A. C.; Maher, R. L.; Bloom, L. B. *DNA Repair* **2005**, *4*, 1088–1098.
(28) Wang, P.; Guliaev, A. B.; Elder, R. H.; Hang, B. *DNA Repair* **2006**, *5*, 23–31.
(29) Maher, R. L.; Vallur, A. C.; Feller, J. A.; Bloom, L. B. *DNA Repair* **2007**, *6*, 71–81.
(30) Lee, C. Y. I.; Delaney, J. C.; Kartalou, M.; Lingaraju, G. M.; Maor-Shoshani, A.; Essigmann, J. M.; Samson, L. D. *Biochemistry* **2009**, *48*, 1850–1861.
(31) Lau, A. Y.; Scharer, O. D.; Samson, L.; Verdine, G. L.; Ellenberger, E. *Cell* **1998**, *95*, 249–258.
(32) Lau, A. Y.; Wyatt, M. D.; Glassner, B. J.; Samson, L. D.; Ellenberger, T. *Proc. Natl. Acad. Sci. U.S.A.* **2000**, *97*, 13573–13578.
(33) Lingaraju, G. M.; Davis, C. A.; Setser, J. W.; Samson, L. D.; Drennan, C. L. *J. Biol. Chem.* **2011**, *286*, 13205–13213.
(34) Rutledge, L. R.; Campbell-Verduyn, L. S.; Wetmore, S. D. *Chem. Phys. Lett.* **2007**, *444*, 167–175.
(35) Rutledge, L. R.; Durst, H. F.; Wetmore, S. D. *Phys. Chem. Chem. Phys.* **2008**, *10*, 2801–2812.
(36) Rutledge, L. R.; Wetmore, S. D. *J. Chem. Theory Comput.* **2008**, *4*, 1768–1780.
(37) Rutledge, L. R.; Durst, H. F.; Wetmore, S. D. *J. Chem. Theory Comput.* **2009**, *5*, 1400–1410.
(38) Lyons, D. M.; O'Brien, P. J. *J. Am. Chem. Soc.* **2009**, *131*, 17742–17743.
(39) Wolfe, A. E.; O'Brien, P. J. *Biochemistry* **2009**, *48*, 11357–11369.
(40) Hendershot, J. M.; Wolfe, A. E.; O'Brien, P. J. *Biochemistry* **2011**, *50*, 1864–1874.
(41) O'Brien, P. J.; Ellenberger, T. *Biochemistry* **2003**, *42*, 12418–12429.
(42) Guliaev, A. B.; Hang, B.; Singer, B. *Nucleic Acids Res.* **2002**, *30*, 3778–3787.
(43) Alexandrova, A. N. *Biophys. Chem.* **2010**, *152*, 118–127.
(44) Sun, X.; Lee, J. K. *J. Org. Chem.* **2007**, *72*, 6548–6555.
(45) Liu, M.; Xu, M.; Lee, J. K. *J. Org. Chem.* **2008**, *73*, 5907–5914.
(46) Case, D. A.; et al. *AMBER 10*; University of California: San Francisco, CA, 2008.
(47) Case, D. A.; et al. *AMBER Tools*, Version 1.0; University of California: San Francisco, CA, 2008.
(48) Cornell, W. D.; Cieplak, P.; Bayly, C. I.; Gould, I. R.; Merz, K. M.; Ferguson, D. M.; Spellmeyer, D. C.; Fox, T.; Caldwell, J. W.; Kollman, P. A. *J. Am. Chem. Soc.* **1995**, *117*, 5179–5197.
(49) Wang, J. M.; Wolf, R. M.; Caldwell, J. W.; Kollman, P. A.; Case, D. A. *J. Comput. Chem.* **2004**, *25*, 1157–1174.
(50) Wang, J.; Wang, W.; Kollman, P. A.; Case, D. A. *J. Mol. Graphics Modell.* **2006**, *25*, 247–260.
(51) Bayly, C. I.; Cieplak, P.; Cornell, W. D.; Kollman, P. A. *J. Phys. Chem.* **1993**, *97*, 10269–10280.

(52) Cornell, W. D.; Cieplak, P.; Bayly, C. I.; Kollman, P. A. *J. Am. Chem. Soc.* **1993**, *115*, 9620–9631.
(53) Vreven, T.; Byun, K. S.; Komaromi, I.; Dapprich, S.; Montgomery, J. A.; Morokuma, K.; Frisch, M. J. *J. Chem. Theory Comput.* **2006**, *2*, 815–826.
(54) Vreven, T.; Frisch, M. J.; Kudin, K. N.; Schlegel, H. B.; Morokuma, K. *Mol. Phys.* **2006**, *104*, 701–714.
(55) Vreven, T.; Morokuma, K. *Annu. Rep. Comput. Chem.* **2006**, *2*, 35–51.
(56) Frisch, M. J.; et al. *Gaussian 09*, revision A.02; Gaussian, Inc.: Wallingford, CT, 2009.
(57) Hirao, H.; Morokuma, K. *J. Am. Chem. Soc.* **2009**, *131*, 17206–17214.
(58) Li, X.; Chung, L. W.; Paneth, P.; Morokuma, K. *J. Am. Chem. Soc.* **2009**, *131*, 5115–5125.
(59) Lill, S. O. N.; Siegbahn, P. E. M. *Biochemistry* **2009**, *48*, 1056–1066.
(60) Maupin, C. M.; McKenna, R.; Silverman, D. N.; Voth, G. A. *J. Am. Chem. Soc.* **2009**, *131*, 7598–7608.
(61) Tao, P.; Fisher, J. F.; Shi, Q.; Vreven, T.; Mobashery, S.; Schlegel, H. B. *Biochemistry* **2009**, *48*, 9839–9847.
(62) Tao, P.; Gatti, D. L.; Schlegel, H. B. *Biochemistry* **2009**, *48*, 11706–11714.
(63) Tomasello, G.; Olaso-Gonzalez, G.; Altoe, P.; Stenta, M.; Serrano-Andres, L.; Merchan, M.; Orlandi, G.; Bottoni, A.; Garavelli, M. *J. Am. Chem. Soc.* **2009**, *131*, 5172–5186.
(64) Bras, N. F.; Fernandes, P. A.; Ramos, M. J. *J. Chem. Theory Comput.* **2010**, *6*, 421–433.
(65) Chung, L. W.; Li, X.; Sugimoto, H.; Shiro, Y.; Morokuma, K. *J. Am. Chem. Soc.* **2010**, *132*, 11993–12005.
(66) Hirao, H.; Morokuma, K. *J. Am. Chem. Soc.* **2010**, *132*, 17901–17909.
(67) Illingworth, C. J. R.; Loenarz, C.; Schofield, C. J.; Domene, C. *Biochemistry* **2010**, *49*, 6936–6944.
(68) Kurland, M. D.; Newcomer, M. B.; Peterlin, Z.; Ryan, K.; Firestein, S.; Batista, V. S. *Biochemistry* **2010**, *49*, 6302–6304.
(69) Sekharan, S.; Altun, A.; Morokuma, K. *J. Am. Chem. Soc.* **2010**, *132*, 15856–15859.
(70) Sekharan, S.; Morokuma, K. *J. Am. Chem. Soc.* **2011**, *133*, 4734–4737.
(71) Shi, Q.; Meroueh, S. O.; Fisher, J. F.; Mobashery, S. *J. Am. Chem. Soc.* **2011**, *133*, 5274–5283.
(72) Rutledge, L. R.; Wetmore, S. D. *Can. J. Chem.* **2010**, *88*, 815–830.
(73) Zhao, Y.; Truhlar, D. G. *Theor. Chem. Acc.* **2008**, *120*, 215–241.
(74) Tao, P.; Schlegel, H. B. *J. Comput. Chem.* **2010**, *31*, 2363–2369.
(75) Przybylski, J. L.; Wetmore, S. D. *Biochemistry* **2011**, *50*, 4218–4227.
(76) Stacking and T-shaped interaction distances (in Å) are measured between heavy atom ring centroids (Y127, H136, or Y159) and the nucleobase heavy atom ring plane, and angles (in degrees) are measured between heavy atom ring planes (nucleobase and Y127, H136, or Y159).
(77) Sherrill, C. D.; Takatani, T.; Hohenstein, E. G. *J. Phys. Chem. A* **2009**, *113*, 10146–10159.
(78) Singer, B.; Antoccia, A.; Basu, A. K.; Dosanjh, M. K.; Fraenkelconrat, H.; Gallagher, P. E.; Kusmierek, J. T.; Qiu, Z. H.; Rydberg, B. *Proc. Natl. Acad. Sci. U.S.A.* **1992**, *89*, 9386–9390.
(79) Lindahl, T. *Nature (London, U. K.)* **1993**, *362*, 709–715.
(80) Zoltewicz, J. A.; Clark, D. F.; Sharpless, T. W.; Grahe, G. *J. Am. Chem. Soc.* **1970**, *92*, 1741–&.
(81) Lindahl, T.; Nyberg, B. *Biochemistry* **1972**, *11*, 3610–3618.
(82) Parkin, D. W.; Leung, H. B.; Schramm, V. L. *J. Biol. Chem.* **1984**, *259*, 9411–9417.
(83) Parkin, D. W.; Schramm, V. L. *Biochemistry* **1987**, *26*, 913–920.
(84) Barnes, J. A.; Williams, I. H. *Chem. Commun.* **1996**, 193–194.
(85) Berti, P. J.; Schramm, V. L. *J. Am. Chem. Soc.* **1997**, *119*, 12069–12078.
(86) McCann, J. A. B.; Berti, P. J. *J. Am. Chem. Soc.* **2007**, *129*, 7055–7064.
(87) Rios-Font, R.; Rodriguez-Santiago, L.; Bertran, J.; Sodupe, M. *J. Phys. Chem. B* **2007**, *111*, 6071–6077.
(88) Schroeder, G. K.; Wolfenden, R. *Biochemistry* **2007**, *46*, 13638–13647.
(89) Przybylski, J. L.; Wetmore, S. D. *J. Phys. Chem. B* **2010**, *114*, 1104–1113.
(90) Shishkin, O. V.; Dopieralski, P.; Palamarchuk, G. V.; Latajka, Z. *Chem. Phys. Lett.* **2010**, *490*, 221–225.
(91) Rios-Font, R.; Bertran, J.; Sodupe, M.; Rodriguez-Santiago, L. *Theor. Chem. Acc.* **2011**, *128*, 619–626.
(92) Werner, R. M.; Stivers, J. T. *Biochemistry* **2000**, *39*, 14054–14064.
(93) McCann, J. A. B.; Berti, P. J. *J. Am. Chem. Soc.* **2008**, *130*, 5789–5797.
(94) Scharer, O. D.; Nash, H. M.; Jiricny, J.; Laval, J.; Verdine, G. L. *J. Biol. Chem.* **1998**, *273*, 8592–8597.
(95) Birck, M. R.; Schramm, V. L. *J. Am. Chem. Soc.* **2004**, *126*, 2447–2453.
(96) Yip, V. L. Y.; Varrot, A.; Davies, G. J.; Rajan, S. S.; Yang, X. J.; Thompson, J.; Anderson, W. F.; Withers, S. G. *J. Am. Chem. Soc.* **2004**, *126*, 8354–8355.
(97) We note that it could be of interest to complete the Y127F and Y159F mutations in attempts to separate the contributions of the $\pi-\pi$ and hydrogen-bonding interactions. However, because we are ultimately interested in the effect of the relevant $\pi-\pi$ interaction (TYR−substrate) on the excision barrier, which would not be properly represented with the mutation to an unpolarized π-ring (Phe−substrate interaction), these mutations were not considered in the present work.
(98) Hedglin, M.; O'Brien, P. J. *Biochemistry* **2008**, *47*, 11434–11445.
(99) Hedglin, M.; O'Brien, P. J. *ACS Chem. Biol.* **2010**, *5*, 427–436.
(100) This was calculated as the difference between the constrained ONIOM(M06-2X/6-31G(d):AMBER) reaction barriers where Wat13 is present and Wat13 was deleted. To obtain the reaction barrier upon deletion of Wat13, the constrained stationary points were not further optimized. Specifically, charges were obtained directly following Wat13 deletion and used in a subsequent single-point calculation.
(101) Singh, V.; Schramm, V. L. *J. Am. Chem. Soc.* **2006**, *128*, 14691–14696.
(102) Versees, W.; Loverix, S.; Vandemeulebroucke, A.; Geerlings, P.; Steyaert, J. *J. Mol. Biol.* **2004**, *338*, 1–6.